Proc. NIPR Symp. Upper Atmos. Phys., 7, 1–12, 1994

# ION TEMPERATURE IN THE POLAR CAP OBSERVED BY SUPRATHERMAL ION MASS SPECTROMETER ON AKEBONO SATELLITE

Eiichi SAGAWA[1] and Shigeto WATANABE[2]

[1]*Communications Research Laboratory, 2–1, Nukuikitamachi 4-chome, Koganei-shi, Tokyo 184*
[2]*Hokkaido Institute of Information, 45, Nishinopporo, Ebetsu 069*

***Abstract:*** Mass resolved ion temperatures in the polar cap at altitudes between 2000 and 10000 km are studied statistically based on observations made by Suprathermal ion Mass Spectrometer (SMS) on the Akebono satellite. Ion temperature is obtained by calculating the zeroth, first, and second order moments of two-dimensional ion distribution functions. The method provides not only ion temperature but also parallel and perpendicular temperatures with respect to the magnetic field, by assuming a bi-Maxwellian distribution. Also, the moment calculation provides other plasma quantities such as density and drift velocities. The statistical analysis uses the SMS data acquired over the northern polar region for almost three years. Average altitude profiles of ion temperature for $H^+$, $He^+$, and $O^+$ ions decrease with the increase of altitude up to about 6000 km, and above this altitude ion temperature becomes constant or shows a slight increase with altitude. The ratio $T_{\parallel}/T_{\perp}$ is almost 1.0 for $H^+$, while this number increases with ion mass below 6000 km. The difference is due to the higher $T_{\perp}$ for $H^+$ than other ions, and suggests strong frictional heating of $H^+$ ions under the polar wind condition.

## 1. Introduction

Thermal structure of the ionosphere is greatly affected by the ionosphere-magnetosphere coupling in the polar region. In the auroral region, strong and time varying precipitation of the magnetospheric particles modifies the ionosphere considerably. Besides this, the fact that the field lines in the polar region are open to the magnetosphere causes a major effect on the thermal structure of the polar ionosphere. The open field lines produce the fast-moving light ions ("Polar Wind") through the background plasma, and also allow the hot magnetosphere to be connected directly to the cold ionosphere. Many theoretical models have predicted the thermal structure of the ionosphere above ~2000 km under the Polar Wind condition. From the kinetic approach that is valid in the collisionless limit, it is shown that an ion keeps its first adiabatic invariant when it travels up along a field line, resulting in the reduction of perpendicular energy in proportion to the local magnetic field strength (HOLTZER *et al.*, 1971). SCHUNK and WATKINS (1981, 1982) calculated the parallel and perpendicular ion temperatures and heat flow, along with the flow velocity and density distributions by using generalized transport equations. They show that, although there is an appreciable temperature anisotropy with $T_{i\parallel}>T_{i\perp}$, the anisotropy is much smaller than predicted by earlier models in the collisionless regime at altitudes above 2000 km. A recent approach to the "Polar Wind" problem

uses the semi-kinetic technique that includes effects of the "small-angle Coulomb collisions" (WILSON *et al.*, 1992), and its results show a complex thermal structure in the polar wind ionosphere due to competing heating and cooling processes.

Another effect of the open field line comes from the direct connection with the hot magnetosphere. Several attempts have been made to evaluate this effect on the polar ionosphere. It is suggested that, with enough magnetospheric hot electrons precipitating into the ionosphere, ion temperature and plasma density will have a sharp transition in their altitude profiles (BARAKAT and SCHUNK, 1984; HO *et al.*, 1992). This sharp transition corresponds to a contact surface between the magnetosphere and ionosphere.

Although several important advances have been made in simulation of the high altitude polar ionosphere, observations of plasma parameters in this region have not been accumulated up to the point where comparisons between simulations and observations improve our understanding of the polar ionosphere. This is particularly true in the case of ion temperature. The suprathermal Ion Mass Spectrometer (SMS) on board the Akebono satellite measures the mass-resolved ion distribution function of thermal ions in the polar ionosphere at altitudes between 300 and 10000 km. Since we have operated SMS for more than three years, it is now possible to analyze the SMS data to obtain an average picture of the polar ionosphere. This paper reports preliminary results of statistical study of ion temperature in the polar ionosphere, in addition to a brief description of the data analysis method to derive ion temperature and other plasma parameters from the individual SMS observation. In the next section, we briefly discuss instrumentation and the data analysis method, followed with an example of SMS data. Then, the description of data and results of statistical study are presented.

## 2. Data Analysis

The scientific goal of the SMS instrument is to provide new observations of the thermal and suprathermal ion population in the Earth's high-latitude magnetosphere. In order to achieve this goal, the design of the instrument features extension of its energy range down to 1 eV and measurements of two-dimensional ion distribution function. The SMS instrument is a radio-frequency type ion mass spectrometer that was designed to measure the major as well as minor ion constituents of the magnetospheric ion population. The instrument energy range extends from less than 1 eV up to 4 keV which includes the thermal as well as the suprathermal ion population. The instrument is mounted on the satellite so as to look out perpendicular to the spin axis. This configuration makes it possible for the instrument to obtain the two-dimensional ion distribution function in the plane perpendicular to the spin axis. Details of the instrument are given in WHALEN *et al.* (1990).

SMS has various modes of operation to organize its measurements and telemetry data. Modes can be divided into two groups, one (FAST mode) which has faster energy and spin angle scan rate but only for fixed number of ion masss (typically four). In the other group of modes (MASS mode), a complete ion mass scan is done between 1 to 64 amu/q with limited time resolution. In this analysis, we used only

the data taken in the FAST mode, where RPA curves for four ion species ($H^+$, $He^+$, $O^+$, $O^{++}$) are measured in the thermal energy range up to 25 V. The sequence is repeated 32 times per one satellite spin (about 8 s). Then, the instrument measures the suprathermal ions during the next spin period. In this analysis, only the thermal ion data are used to calculate ion temperature.

The raw data obtained with the instrument are a collection of RPA curves, which are the incoming ion fluxes corresponding to the retarding potential voltage. Therefore, derivatives of these curves give differential flux at the energy which is equivalent to the retarding potential plus potential of the satellite with respect to the ambient plasma. From the differential fluxes measured in the satellite spin plane, two-dimensional ion distribution function $f_m$ ($V$, $\phi$) can be constructed, where $V$ and $\phi$ are particle velocity and the spin phase angle, respectively. During the course of data reduction, the satellite potential was estimated by assuming that all ion species have a common drift velocity perpendicular to the local magnetic field. Details of this procedure and derivations of plasma parameters based on the moment calculation are given in WATANABE *et al.* (1992). We, in this analysis, added calculations of parallel and perpendicular temperatures with respect to the field line, as shown in the following set of equations:

$$T_{\parallel}(m) = m/2kN(m) \int (\vec{V} - \vec{V}_o)_{\parallel}^2 f_m (V, \phi) V \, dV \, d\phi, \tag{1}$$

$$T_{\perp}(m) = m/2kN(m) \int (\vec{V} - \vec{V}_o)_{\perp}^2 f_m (V, \phi) V \, dV \, d\phi, \tag{2}$$

where, $N(m)$, $V_o(m)$, $T_{\parallel}(m)$ and $T_{\perp}(m)$ are density, plasma drift velocity, and field-parallel and perpendicular temperatures for ion $m$, respectively. It should be noted that the two-dimensional distribution function $f_m(V, \phi)$ observed by SMS is in the plane perpendicular to the spin axis, which does not necessarily contain the local field lines. This is due to attitude control of the satellite, which keeps the spin axis directed toward the sun, so that the SMS's ion distribution function does not cover the full 0° to 180° pitch angle space. However, over the polar region, this coverage is generally good, and in the statistical study to be presented later in this paper, we only use data that covered good pitch angle range.

Figure 1 shows an example of the two-dimensional ion distribution function measured by SMS. Four panels indicate ion distribution functions for $H^+$, $He^+$, $O^{++}$, and $O^+$ in the satellite spin plane. Note that the spin plane does not necessarily include the local magetic field line, and that the X (labeled as $V_{para}$) and Y ($V_{perp}$) axes are defined so that the parallel axis corresponds to the minimum and maximum pitch angle direction during one satellite spin. The vertical dashed line in each panel indicates the spacecraft velocity projected on the $V_{para}$ axis, while the horizontal line shows the spacecraft velocity plus perpendicular drift velocity estimated from the SMS data. Dots show the sampling point. The figure shows several noteworthy features. First, all distributions are centered at the location shifted from the parallel velocity of the spacecraft toward the positive $V_{para}$ direction. Amounts of these shifts correspond to their drift velocities along field lines. The drift velocity is the largest for $H^+$, and the minimum for $O^+$. The second point is that the $O^+$ distribution

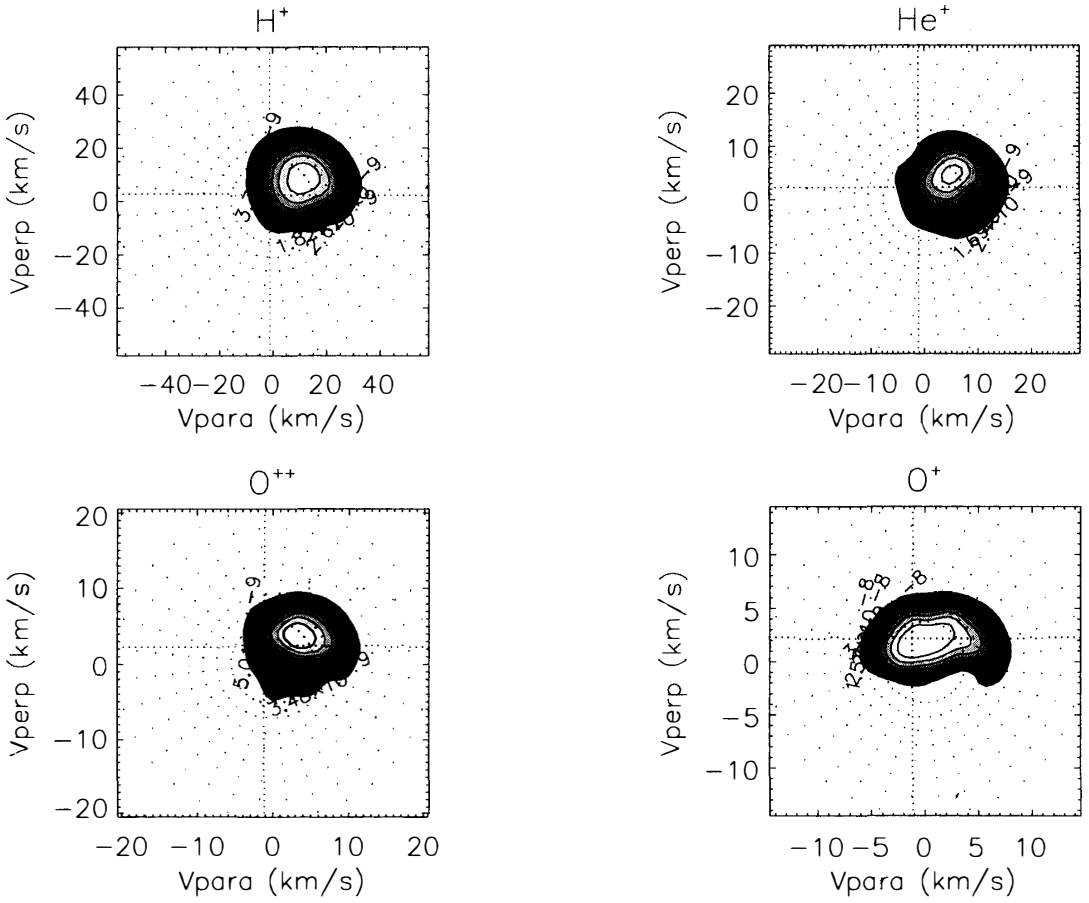


*Fig. 1. Ion distribution functions observed by SMS. Four panels corresponds to four ion species indicated at the top of each panel. The data were taken on September 21, 1992, 0424 UT over the Syowa Station. The satellite was located at 80.4° Inv. and 0630 MLT.*

shows significant amount of anisotropy, while other ions show more or less circular distribution. This suggests that $O^+$ ions have significant temperature anisotropy, while other ions have fairly isotropic Maxwell distributions.

As described by WATANABE *et al.* (1992), various plasma parameters can be calculated from ion distribution functions shown above. For example, plasma parameters calculated for Fig. 1 are shown in Table 1. Figure 2 plots, from top to bottom, perpendicular and parallel drift velocities ($V^i_\perp$, $V^i_\parallel$), ion densities ($N^i$), ion tempera-

*Table 1. Plasma parameters estimated from ion distribution function shown in Fig. 1. Note that $V_\perp$ is assumed to be common for all three ions to estimate the satellite potential.*

| | $N_i$ (cm$^{-3}$) | $T^i$ (K) | $T^i_\parallel$ (K) | $T^i_\perp$ (K) | $V_\parallel$ (km/s) | $V_\perp$ (km/s) |
|---|---|---|---|---|---|---|
| $H^+$ | 0.05 | 4000 | 3600 | 4300 | 9.2 | |
| $He^+$ | 0.007 | 4800 | 5200 | 4600 | 4.7 | 0.73 |
| $O^{++}$ | 0.007 | 5600 | 5700 | 5600 | 3.2 | |
| $O^+$ | 0.013 | 5600 | 7000 | 4300 | 2.2 | |

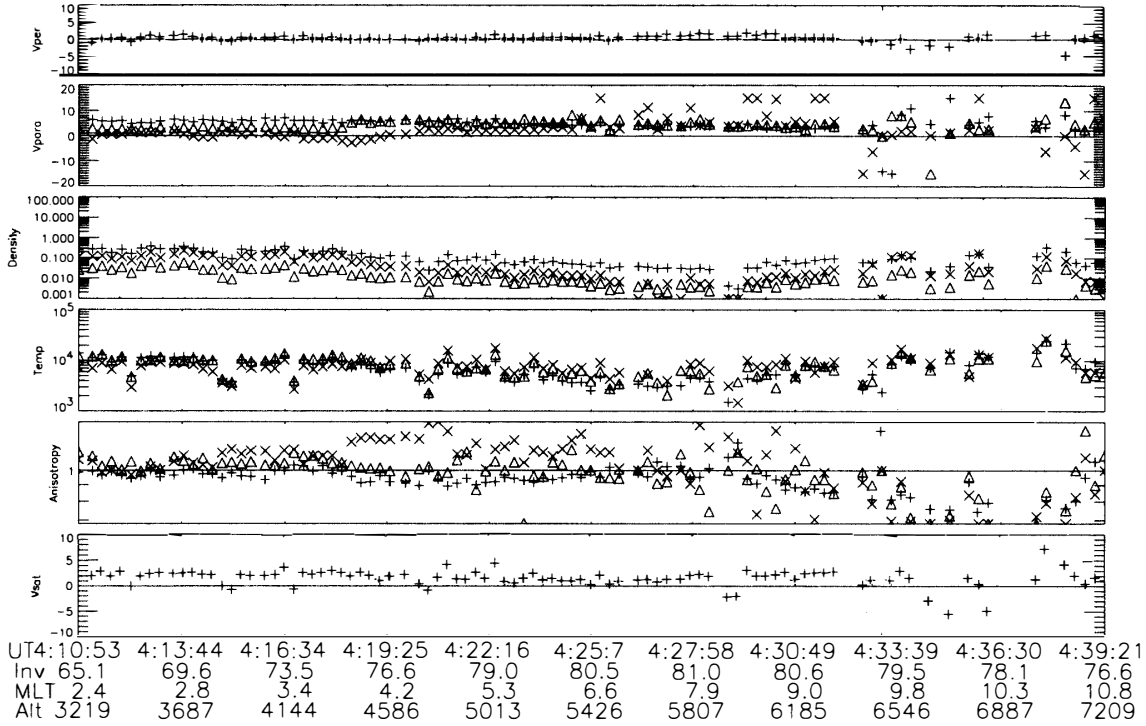


*Fig. 2. Summary plot of plasma parameters observed by SMS. Six panels are, from top to bottom, $V_\perp$, $V^i_\parallel$, $N^i$, $T^i$, $T^i_\parallel/T^i_\perp$, and satellite potential. The three symbols +, △, × correspond to $H^+$, $He^+$, and $O^+$, respectively, for $V^i_\parallel$, density, temperature, and anisotropy plots. The observation was made over the Syowa Station on September 21, 1990 (same as Fig. 1).*

tures ($T^i$), ion temperature anisotropy defined as $T^i_\parallel/T^i_\perp$, and satellite potential for about 20-minute segments of the satellite path over Syowa Station on September 21, 1990. $V^i_\parallel$, density, temperature, and anisotropy are shown for three ion species of $H^+$, $He^+$, $O^+$. During the period presented here, the satellite was traveling from low to high latitudes in the morning sector, and from low to high altitudes (3300 to 6700 km). The second panel indicates that filed-parallel drift velocity of $H^+$ is less than 10 km/s and remains almost constant, except that after 0425 UT data become somewhat scattered due to the low signal to noise ratio. $He^+$ drift velocity behaved differently. At first, it was almost zero. Then, around 0418 UT, drift velocity became upward, and stayed around 5 km/s. Also observed was a small upward motion of $O^+$ ions after 0421 UT. These field-aligned plasma drift were correspond to the "Polar Wind". Ion temperatures for all three ions were approximately 10000 K at first, and decreased slightly with time. However, anisotropy of ion temperature (fifth panel) is noticeable for $O^+$ ions after 0414 UT. It increased with time, and became larger than 2 around 0418 UT. The ion distribution functions shown in Fig. 1 were obtained at 0424 UT, and indicate large anisotropy of $O^+$ ions.

## 3. Statistical Results

SMS has been observing the polar ionosphere for more than three years since the launch of the Akebono satellite in February 1989. However, data processing does not really catch up with the data telemetry rate. We have mostly processed the data observed over the northern hemisphere from November 1989 to December 1992. In addition, we just started processing data acquired over the southern hemisphere. The data used in this statistical analysis came from observations over the northern hemisphere. We have set up several rules of data selection for statistical analysis to minimize possible errors; that is, we have used

1) Only data taken at invariant latitudes higher than 80°, and
2) Only data taken when the pitch angle coverage is better than 150°.

The first rule is used to avoid effects of auroral activity such as ion conics and ion beams that are frequently seen in the auroral oval. Because our method of plasma parameter calculation reflects an average over the total ion distribution function, addition of non-thermal components associated with those phenomena should be avoided. In addition, by limiting ourselves to the invariant latitude above 80°, we intend to simplify the statistical analysis. The polar ionosphere is under the control of both magnetospheric and ionospheric processes. For example, effects due to the magnetosphere may be best described with the magnetic local time (MLT) and invariant latitude coordinate, while the effect of the sun is dependent on the local time. Therefore, in this study, we focused on the altitude profile of a plasma parameter.

The second rule is to make sure we have a good approximation of real distribution function in the pitch angle space, because we are going to discuss field-aligned and field-perpendicular temperatures separately. These two rules resulted in about 4000 data point being available for this analysis. Figure 3 plots these data points in the MLT-Invariant Latitude coordinate. Note that, if the data quality is not good enough to calculate plasma parameters, the data are rejected. This tends to happen when plasma density is low and SMS could not collect enough ions. Also the relatively low density of data points in the noon sector is due to strong heating commonly seen in association with the cusp/cleft region. This heating usually appears as

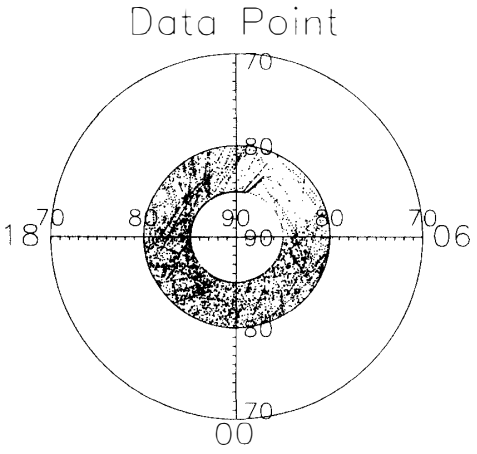


*Fig. 3. Data points used in the statistical study. All data were obtained over the northern polar region.*

transverse ion heating or ion conics, and it is not possible to estimate bulk plasma parameters by using the same technique we used in this analysis. Even the data with low quality are rejected; still, there is a large scatter of plasma parameters at high altitudes. Currently we think that the low plasma density is part of the reason for the large fluctuation of plasma parameters at higher altitudes, as seen in Fig. 2. However, it is possible that our rules of data selection are not strict enough for study of the unperturbed ionosphere. This point should be addressed in the future study.

By limiting ourselves to the data above 80°, we ignore the dependence on the magnetic local time, and we only take the altitude as a parameter. Figures 4 and 5 plot average altitude profiles of $T^i$, $V^i_\parallel$, $N^i$, $T^i_\parallel$, $T^i_\perp$, and anisotropy defined as $T^i_\parallel/T^i_\perp$ for three ion species ($H^+$, $He^+$, and $O^+$ from left to right). Error bars are given as $\pm\sigma$. As shown in Fig. 4, ion temperature is in the range between 4000 and 10000 K, except in the lowest altitude bin. The high ion temperature in the lowest altitude bin is probably due to the saturation effect of the instrument in the high plasma density region. The saturation of ion count tends to result in temperature higher than the actual one because the ion distribution function is broader than the actual one. Except for the lowest two altitude bins, ion temperature for all three ion species decreases with increasing altitude. Note that error bars tend to be large above 5000 km, partly due to low ion flux. The middle panels of Fig. 4 show field-aligned ion drift velocities, in which negative velocity corresponds to the upward drift because the field lines are directed toward the Earth in the northern hemisphere where those

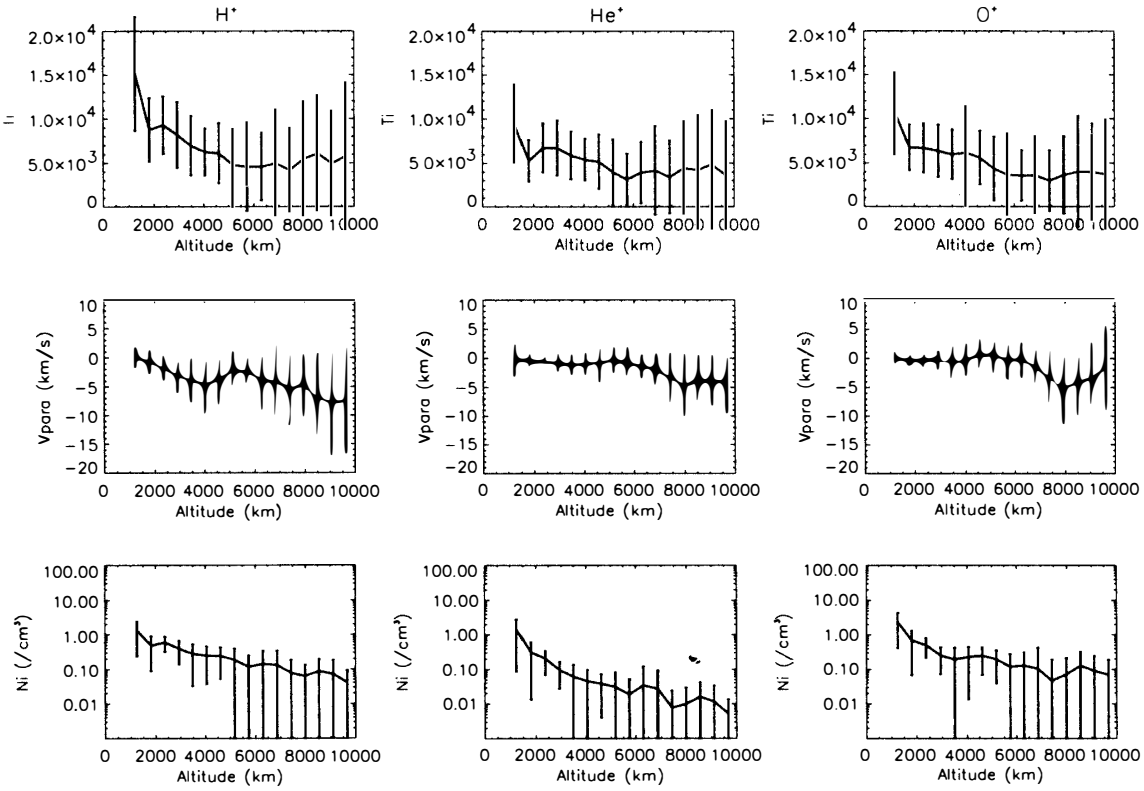


*Fig. 4. Average altitude profiles of $T^i$, $V^i_\parallel$, and $N^i$ (top to bottom) for $H^+$, $He^+$, and $O^+$ (left to right).*

data were obtained. Note that observations shown in Figs. 1 and 2 were done over the southern polar region where positive drift velocity corresponds to the upward drift. It is clear in the figure that the $H^+$ upward drift velocity increases with increasing altitude, although $He^+$ and $O^+$ have an appreciable upward velocity at higher altitudes. These characteristics are fully described in ABE *et al.* (1993), and are not repeated here. Note that, because we have not compensated for the change in the absolute detection efficiency of the instrument during three years of operation, number density data given here are not final and are therefore discussed here. A change of absolute efficiency, however, would not affect calculation of drift velocities and temperatures.

Parallel and perpendicular temperatures shown in Fig. 5 show similar behavior to ion temperature shown in Fig. 4. However, anisotropy shown at the bottom of the figure suggests that there is a slight difference between parallel and perpendicular temperatures, particularly for $O^+$ ions. At altitude below 5000 km, temperature anisotropy of $O^+$ ions increases with increasing altitude. Above this altitude, it decreases slowly with altitude. In order to make comparison of ion temperatures of different ion species more clear, Figs. 6–8 plot $T^i_{\parallel}$, $T^i_{\perp}$, and and anisotropy for three ions. As for $T^i_{\parallel}$ and shown in Fig. 6, $H^+$ has the highest temperature below about 3000 km. However, between 3000 and 6000 km, $T^{O+}_{\parallel}$ is highest, and, above 6000 km, all three ions have comparable temperature. On the other hand, $T^{O+}_{\perp}$ is consistently higher than the other two ion species below 6000 km (Fig. 7). Figure 8

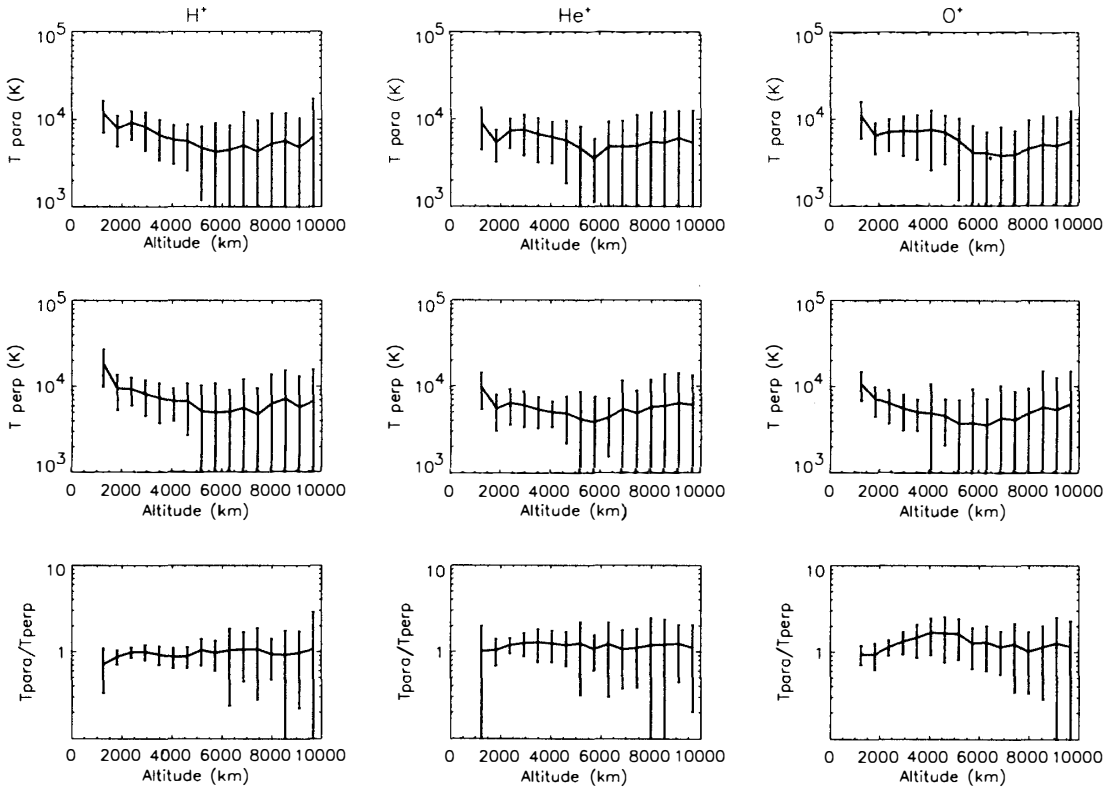


*Fig. 5. Average altitude profiles of $T^i_{\parallel}$, $T^i_{\perp}$, and anisotropy defined as $T^i_{\parallel}/T^i_{\perp}$ (top to bottom) for $H^+$, $He^+$, and $O^+$ (left to right).*

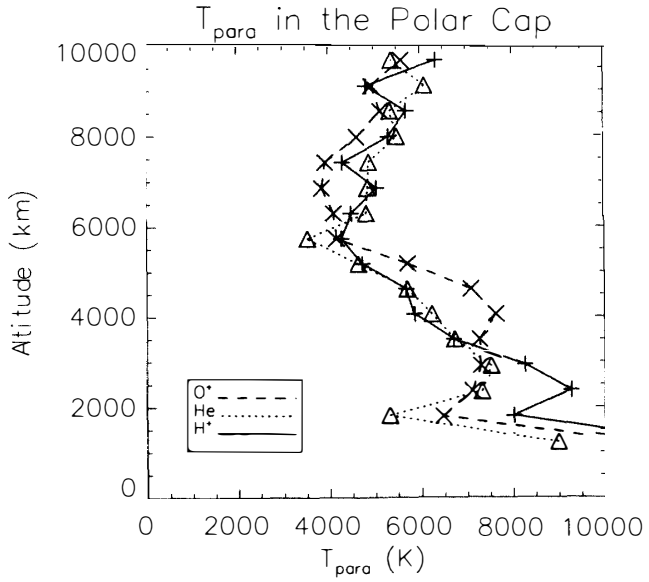


*Fig. 6. Altitude profiles of $T_{\|}$ for three ions.*

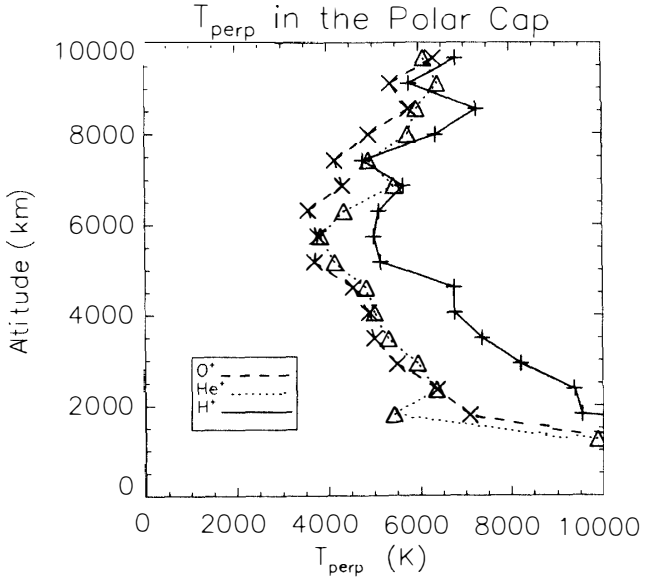


*Fig. 7. Altitude profiles of $T_{\perp}$ for three ions.*

reflects these features which appear in altitude profiles of $T_{\|}^{i}$ and $T_{\perp}^{i}$. $O^+$ has the highest anisotropy at altitudes around 5000 km due to higher $T_{\|}^{O+}$ than the other two ions, while the higher $T_{\perp}^{H+}$ causes the lower anisotropy for $H^+$.

## 4. Summary and Discussion

More than three years of SMS observations over the northern polar region enable us to analyze average altitude profiles of ion temperature in the polar cap.

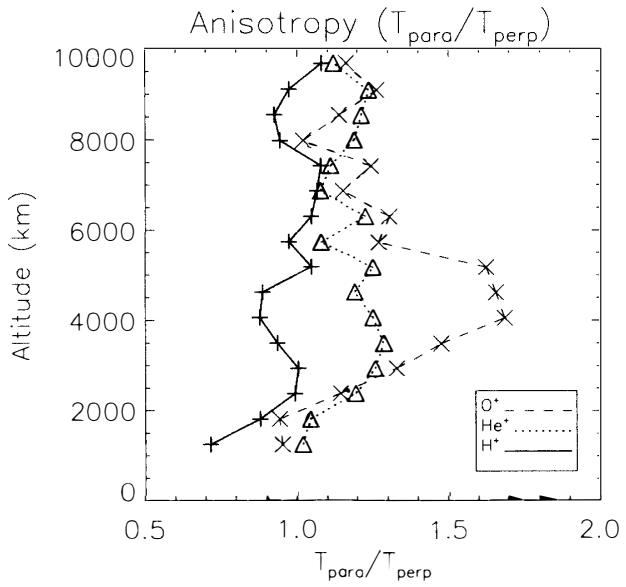


*Fig. 8. Altitude profiles of $T_{\parallel}/T_{\perp}$ for three ions.*

Although our analysis is still in a preliminary stage for lack of important geophysical conditions such as *Kp* and IMF, there are several important findings in the altitude profiles of ion temperature presented:

a) Average ion temperature in the polar cap at altitudes from 2000 and 10000 km is in the range between 5000 to 10000 K, although a large fluctuation is seen at higher altitudes.

b) Between 2000 and 6000 km, ion temperature decreases with increasing altitude.

c) Ion temperatures for all ions are almost constant or show slight increase above 6000 km.

d) There is an appreciable amount of ion temperature anisotropy between 2000 and 6000 km for $O^+$.

e) $H^+$ ion has higher $T_{\perp}$ compared to the other two ions.

There have been few observation of ion temperature at several thousand km altitudes in the polar cap region. Measurements with the Langmuir probe or with the conventional RPA method would not work correctly in this region because of low plasma density. The only possible method to determine ion temperature is to measure ion distribution function directly by a particle detector. However, most particle detectors flown before have an energy range much higher than thermal ions. The RIMS instrument on the DE-1 satellite was also designed to measure thermal ion distribution function by using the highly sensitive technique of particle detection. Although, the instrument was not fully functional to measure full ion distribution function, several sets of ion temperature data have been published based on DE-1/RIMS data (COMFORT *et al.*, 1987; CHANDLER *et al.*, 1987; COMFORT *et al.*, 1988). Because those ion temperature data are limited to the outer plasmasphere, we could not directly compare our data with DE-1/RIMS results. However, considering the fact that the DE-1/RIMS instrument typically measures ion temperature around

10000 K at about 8000 km (CHANDLER *et al.*, 1987), our result for ion temperature is not incompatible with their results.

Since collisions are not a major factor at altitudes above 2000 km, earlier simulations of the polar wind predicted essentially constant $T_{\parallel}$ and decreasing $T_{\perp}$ with altitude due to conservation of the first adiabatic invariant of each ion, which results in temperature anisotropy growing with altitude (HOLTZER *et al.*, 1971). However, recent simulations by employing a more sophisticated method such as generalized transport equations (SCHUNK and WATKINS, 1982) and semikinetic simulation (WILSON *et al.*, 1992) predict a smaller temperature anisotropy than previous models. Our results given in Fig. 8 show that anisotropy is only significant for $O^+$ ions below 5000 km. By examining Figs. 6–8, $T_{\parallel}^{O+}$ is fairly constant between 2000 and 6000 km, while $T_{\perp}^{O+}$ decreases with altitude. This situation is what the early simulation models predicted as a result of collisionless plasma motion. On the other hand, there is no major $H^+$ anisotropy in our results. This is due to higher $T_{\perp}^{H+}$ compared to the other two ions. Characteristics of $He^+$ ions generally fall between those of $H^+$ and $O^+$ ions. As shown in Fig. 5, $H^+$ ions have large field-aligned velocity (Polar Wind) compared to the other two ions even at altitudes below 5000 km. Therefore, frictional heating may be important at lower altitudes. WILSON (1992) shows, by using semikinetic simulation including effects of small angle Coulomb collisions, altitude profiles of parallel and perpendicular temperatures are determined by several competing cooling and heating terms, and they are fairly dependent on ionosphere models used in the simulation. Frictional heating due to the polar wind $H^+$ heats primarily $H^+$ ions due to mass difference between $H^+$ and $O^+$, while $T_{\parallel}$ and $T_{\perp}$ decrease due to adiabatic cooling and due to the decreasing magnetic field strength, respectively. Therefore, higher $T_{\perp}^{H+}$ shown in our results is thought as a result of frictional heating, while, in the case of $T_{\parallel}^{H+}$, effect of frictional heating is only visible at altitudes below 3000 km, probably due to the adiabatic cooling effect that effectively reduces $T_{\parallel}^{H+}$above 3000 km.

## Acknowledgments

Akebono data have been received by the Institute of Space and Astronautical Science at Kagoshima in Japan and at the ES range in Sweden, and by the National Institute of Polar Research at the Syowa Station in Antarctica, and by the National Research Council Canada at Prince Alberta in Canada. Authors are indebted to members of the Akebono Science team led by Profs. OYA and TSURUDA for their efforts in the satellite operation.

## References

ABE, T., WHALEN, B., YAU, A., HORITA, R. E., WATANABE, S. and SAGAWA, E. (1993): EXOS D (Akebono) Suprathermal Mass Spectrometer observations of the polar wind. J. Geophys. Res., **98**, 11191–11204.

BARAKAT, A. R. and SCHUNK, R. W. (1984): Effects of hot electrons on the polar wind. J. Geophys. Res., **89**, 9771–9784.

CHANDLER, M. O., KOZYRA, J. U., HORWITZ, J. L. and BRACE, L. H. (1988): Modeling of the thermal plasma in the outer plasmasphere-A magnetospheric heat source. Modeling Magnetospheric Plasma, ed. by T. E. Moore and J. H. Waite. Washington, D.C., Am. Geophys. Union, 101–106 (Geophys. Monogr. **44**).

COMFORT, R. H., NEWBERRY, I. T. and CHAPPELL, C. R. (1985): Preliminary statistical survey of plasmaspheric ion properties from observations be DE 1/RIMS. Modeling Magnetospheric Plasma, ed. by T. E. Moore and J. H. Waite. Washington, D.C., Am. Geophys. Union, 107–114 (Geophys. Monogr. **44**).

COMFORT, R. H., WAITE, J. H. and CHAPPELL, C. R. (1988): Ion temperatures from the retarding ion mass spectrometer on DE 1. J. Geophys. Res., **90**, 3475–3486.

Ho, C. W., HORWITZ, J. L. and CHAPPELL, C. R. (1992): Effects of magnetospheric electrons on polar plasma outflow. J. Geophys. Res., **97**, 8425–8438.

HOLTZER, T. E., FEDDER, J. A. and BANKS, P. M. (1971): A comparison of kinetic and hydro-dynamic models of an expanding ion-exosphere. J. Geophys. Res., **76**, 2453–2465.

SCHUNK, R. W. and WATKINS, D. S. (1982): Ion temperature anisotropy in the polar wind. J. Geophys. Res., **87**, 171–180.

SCHUNK, R. W. and WATKINS, D. S. (1981): Electron temperature anisotropy in the polar wind. J. Geophys. Res., **86**, 91–102.

WATANABE, S., WHALEN, B. A. and YAU, A. W. (1992): Thermal ion observations during plasma-sphere depletion and refilling in the plasmaspheric trough. J. Geophys. Res., **97**, 1081–1096.

WHALEN, B. A., BURROWS, J. R., YAU, A. W., PILON, A. M., IWAMOTO, I., MARUBASHI, K., MORI, H., WATANABE, S. and SAGAWA, E. (1990): The suprathermal ion mass spectrometer (SMS) for the AKEBONO spacecraft. J. Geomagn. Geoelectr., **42**, 511–536.

WILSON, G. R. (1992): Semikinetic modeling of the outflow of ionospheric plasma through the topside collisional to collisionless transition region. J. Geophys. Res., **97**, 10551–10567.

WILSON, G. R., HORWITZ, J. L. and LIN, J. (1992): A semikinetic model for early stage plasma-spheric refilling, 1, Effects of Coulomb collisions. J. Geophys. Res., **97**, 1109–1120.

*(Received May 27, 1993; Revised manuscript received August 6, 1993)*